Appl. Phys. B 58, 117–122 (1994)

Applied Physics B Lasers and Optics

Nonlinear Mode Coupling in Doubly Resonant Frequency Doublers

R. Paschotta, K. Fiedler, P. Kürz, J. Mlynek

Universität Konstanz, D-78434 Konstanz, Germany (Tel.: +49-7531/88-3842, Fax: +49-7531/88-3072)

Received 12 July 1993/Accepted 21 October 1993

Abstract. The concept of a doubly resonant frequency doubler can be used for a variety of experiments concerning both classical phenomena like efficient frequency doubling at low power levels and quantum effects like squeezed states of light or Quantum Non Demolition (QND) measurements. In many of these experiments the strength of the nonlinear coupling of fundamental and second-harmonic modes is of crucial importance. First we treat the general theory for the calculation of the coupling parameter κ, which depends not only on properties of the nonlinear material but also on resonator geometry and some optical phases. On this basis we discuss in detail the situation for two different monolithic resonator geometries, namely a linear (standing-wave) and a ring (travelling-wave) cavity. Finally we compare theoretical predictions for these resonators to the experimentally achieved results.

PACS: 42.65.Ky, 42.50.Dv

Second-harmonic generation is one of the most basic processes in nonlinear optics. It was realized early that the efficiency of a continuously operating frequency doubler can be greatly improved by resonant enhancement of the fundamental wave [1, 2], the second-harmonic wave, or both [3]. In the last case we speak of a doubly resonant frequency doubler. While singly resonant doublers can be very efficient at relatively high input-power levels [4], doubly resonant devices are significantly better at low powers. Recently, we have demonstrated a versatile doubly resonant frequency doubler which yields more than 50% efficiency with only a few milliwatts of input power [5].

The first quantum-mechanical treatment of the doubly resonant frequency doubler has been presented by Drummond et al. in 1980 [6]. In the meantime this system has developed to one of the most paradigmatic systems of quantum optics. It was shown that both fundamental and second-harmonic output can be squeezed [7, 18], and, indeed, intensity fluctuations below the shot-noise level could be demonstrated experimentally [8–11]. In addition, both waves show significant quantum correlations [12], and interesting QND properties have been predicted [13].

Good conversion efficiency at low powers, but, particularly, the demonstration and application of the predicted quantum effects require a strong nonlinear coupling of the modes and low losses. In recent years monolithic-resonator concepts have been developed which meet both requirements. Here, the modes are confined by the surfaces of a single crystal; reflection is achieved by dielectric mirror coatings or total internal reflection. It is important to calculate the strength of the nonlinear coupling, so that one can optimize the resonator design and check whether the theoretical potential has been realized experimentally. It is also important to learn about the degradation effects of inhomogeneities and phase changes upon reflections in the resonator. In this paper we give the theoretical framework, use the results to discuss two particularly interesting practical cases, and present experimental results which show that the theoretically possible figures have now been reached in experiments. We also discuss methods to measure the strength of the nonlinear coupling.

1 General Theory

Drummond et al. have introduced a simple model for a doubly resonant frequency doubler. The two modes for the fundamental and second-harmonic wave are described by two mode amplitudes α_1 and α_2, which are normalized so that $|\alpha_i|^2$ is the photon number in mode i ($i = 1, 2$). Then the time evolution of the system is governed by the equations [6]:

$$\dot{\alpha}_1 = -(\gamma_1 + \mathrm{i}\Delta_1)\alpha_1 + \kappa\alpha_1^*\alpha_2 + \varepsilon\,, \tag{1}$$

$$\dot{\alpha}_2 = -(\gamma_2 + \mathrm{i}\Delta_2)\alpha_2 - \frac{1}{2}\kappa\alpha_1^2\,. \tag{2}$$

The parameters γ_i are the reciprocal damping times of the modes, Δ_i the detunings of both modes relative to the carrier frequency of the pump, and ε is proportional to the amplitude of the pump wave. This model has been used to

calculate both the classical and quantum properties of the light resulting from this process.

In this paper we concentrate on the parameter κ, which expresses the strength of the nonlinear coupling between the waves. The goal is to calculate κ in dependence of the experimental parameters.

We describe the spatial dependence of the modes by complex functions $\Psi_1(\mathbf{r})$ and $\Psi_2(\mathbf{r})$, which are proportional to the complex electrical field amplitudes $\tilde{E}_i(\mathbf{r})$ and are normalized by the condition

$$\int |\Psi_i|^2 \mathrm{d}V = 1\,, \tag{3}$$

where the integration expands over the full resonator volume, including parts of the resonator which are not filled with a nonlinear medium.

In SI units the power transfer between both modes caused by the nonlinearity is given by

$$P_{1\to 2} = \left\langle -\int \frac{\mathrm{d}P_2(\mathbf{r},t)}{\mathrm{d}t}\, E_2(\mathbf{r},t)\mathrm{d}V \right\rangle_t \tag{4}$$

with complex electric field amplitudes

$$E_i(\mathbf{r},t) = \mathrm{Re}(\tilde{E}_i(\mathbf{r})\mathrm{e}^{\mathrm{i}\omega_i t})\,, \tag{5}$$

and nonlinear polarization $P_2(\mathbf{r},t)$, which finally results in

$$P_{1\to 2} = \varepsilon_0 d_{\mathrm{eff}}\omega_1 \left| \int \tilde{E}_1^2(\mathbf{r})\tilde{E}_2^*(\mathbf{r})\mathrm{d}V \right| \tag{6}$$

for the case that the phases between both modes are optimal for energy transfer from the fundamental to the second-harmonic wave. d_{eff} is the relevant component of the nonlinear tensor of the crystal in units of m/V. On the other hand, from (1) and (2) we obtain

$$P_{1\to 2} = 2\hbar\omega_1\kappa|\alpha_1^2\alpha_2| \tag{7}$$

for the same situation. Comparison of (6) and (7) leads to the general formula

$$\kappa = \frac{2d_{\mathrm{eff}}}{n^3}\left(\frac{\hbar\omega_1^3}{\varepsilon_0}\right)^{\frac{1}{2}} \left| \int \Psi_2^*\Psi_1^2\,\mathrm{d}V \right|, \tag{8}$$

which was already given in [6] and [14] in a similar form. Here, the integration is restricted to the nonlinear medium with effective nonlinearity d_{eff} in the cavity. n is the index of refraction which is assumed to be equal for both waves (type-I phase matching).

Now we have to note that the integral depends on the particular set of modes chosen for the fundamental and second-harmonic wave. We only consider axial and no higher-order transverse modes. If we use different axial modes of the second-harmonic wave together with one fixed mode of the fundamental wave, we obtain a series of values κ_N with an integer index N indicating the particular double-resonance (the slight change of κ over the width of one double-resonance can in general be ignored). Only a limited number of double-resonances will have a nonlinear coupling of considerable strength, since for the others the integrand in (8) oscillates rapidly. This can be expressed by the phase-matching condition $k_2 - 2k_1 = 0$, which can be fulfilled approximately only by a few resonances. We choose the index $N = 0$ for the resonance with the strongest coupling. If we switch to one of the adjacent modes for the fundamental wave, we will obtain nearly the same series of values κ_N, only shifted by two resonances of the second-harmonic wave.

For the experiment, we will in general select only the double-resonance with the strongest coupling by starting at the phase-matching temperature of the nonlinear crystal. The detailed pattern of values κ_N can, however, provide useful information for the characterization of the resonator, obviously much more than the comparison of a single number.

2 Theory and Experiment for Particular Resonators

In our experiments we have used two different resonator geometries. One of them is a standing-wave resonator with dielectric mirror coatings. We also have investigated a monolithic ring-resonator geometry with frustrated input/output coupling, which allows one to adjust the reflectivities for both modes in the experiment. In the following we look in detail at the nonlinear coupling for these geometries.

2.1 Monolithic Standing-Wave Resonator

The simplest case is that of a symmetrical standing-wave resonator consisting of a nonlinear crystal of length L. Dielectric mirror coatings are directly evaporated onto the curved end faces with radius of curvature R. This leads to Gaussian modes [15] with a focusing parameter $\xi = (2R/L - 1)^{-1/2}$ and beam waists $w_{0i} = (L\lambda_i/2\pi n\xi)^{1/2}$, where n is the refractive index (which is approximately the same for both waves, since we assume type-I phase matching). The standing-wave fields consist of two components travelling in opposite directions, where the phase relations between those waves depend on the properties of the mirror coatings and is, in general, different for the fundamental and second-harmonic mode. One of the components is described by a complex field distribution

$$E \sim \frac{1}{1+\mathrm{i}z/z_{\mathrm{R}}}\,\mathrm{e}^{\mathrm{i}kz}\exp\left(-\frac{r^2}{w_0^2(1+\mathrm{i}z/z_{\mathrm{R}})}\right) \tag{9}$$

(low round-trip losses are assumed) with the Rayleigh length $z_{\mathrm{R}} = L/2\xi$. We denote the phase changes upon reflection at both sides of the resonator as Φ_{Ai}, Φ_{Bi} and define the relative phase changes $\Delta\Phi_A = 2\Phi_{A2} - \Phi_{A1}$ and $\Delta\Phi_B = 2\Phi_{B2} - \Phi_{B1}$. For double-resonances, the total phase changes per round trip must fulfil the conditions

$$2k_iL - 4\arctan\xi + \Phi_{Ai} + \Phi_{Bi} = M_i 2\pi\,, \tag{10}$$

where the integers M_1, M_2 are related to N by $N = 2M_1 - M_2 + \mathrm{const}$. The term with $\arctan\xi$ results from focusing [15]. When evaluating the overlap integral in (8), we note that the mixed terms between different counterpropagating components are oscillating rapidly and therefore do not significantly contribute to the integral.

Finally, we end up with the result

$$\kappa_N = \frac{d_{\text{eff}}}{n^3}\left(\frac{\hbar\omega_1^3}{\varepsilon_0 V}\right)^{\frac{1}{2}}\frac{\pi}{\xi}\,|H(\sigma_N,\xi)| \times 2^{-3/2}\left|1+\exp\left\{\mathrm{i}\left[N\pi+\frac{1}{2}(\Delta\Phi_B-\Delta\Phi_A)\right]\right\}\right| \quad (11)$$

(again in SI units) with the function

$$H(\sigma,\xi)=\int_{-\xi}^{\xi}\frac{\mathrm{e}^{\mathrm{i}\sigma\tau}}{1+\mathrm{i}\tau}\,\mathrm{d}\tau\,, \quad (12)$$

defined as in [16]. The appearance of the mode volume $V=\pi\omega_0^2 L/2$ results from normalization. The parameter

$$\sigma_N=\Delta k_N z_{\mathrm{R}}=\frac{\arctan\xi}{\xi} + \frac{1}{4\xi}\left[2\pi N-(\Delta\Phi_A+\Delta\Phi_B)\right] \quad (13)$$

indicates the deviation from the phase-matching condition $\Delta k := 2k_1 - k_2 = 0$ for the particular double-resonance N. $\Delta\Phi_A$ and $\Delta\Phi_B$, which are unique only modulo 2π, should be chosen so that κ_0 is the maximum of all κ_N.

The last two factors in (11) do not appear in a result given in [14], where obviously the back-propagating components have been ignored.

A discussion of (11) is instructive. The properties of the nonlinear medium (apart from inhomogeneities) appear in the first factor only. The following terms reflect essentially the geometric factors and also depend on N via σ_N. The last factor shows an interference between the contributions from both counterpropagating waves; for some double-resonances it may become very small. For equal relative phase changes at both mirror coatings one sees that there is totally destructive interference for all resonances with odd N.

The relative contribution of infitesimal cross sections of the crystal (perpendicular to the axis of beam propagation) to the nonlinear coupling is plotted in Fig. 1 ($N = 0$) and Fig. 2 ($N = 2$) for zero phase changes upon reflections. It is basically given by the real part of the integrand in (8), integrated over the beam cross-sections, if the phase between Ψ_1 and Ψ_2 is chosen so that the integral is real and positive.

The optimum of κ_0 with respect to the focusing factor ξ is in general *not* achieved with the well-known value 2.84 derived in [16] for single-pass Second-Harmonic Generation (SHG), unless σ_0 is optimized by proper choice of the relative phase changes $\Delta\Phi_{A,B}$ at the mirrors.

For reasonable parameters we have found that the optimum for $\Delta\Phi_{A,B}$ lies near zero. On the other hand, we have seen from numerical evaluation that the influence of these phase changes is not crucial – even without optimization of the phase changes one would loose less than about a third of the optimum coupling in most cases. This was not obvious but can be explained by the fact that if the coupling for one particular double-resonance is reduced by more than about one third due to large phase changes at the mirrors, the coupling for some other resonance will increase and overtake the optimum.

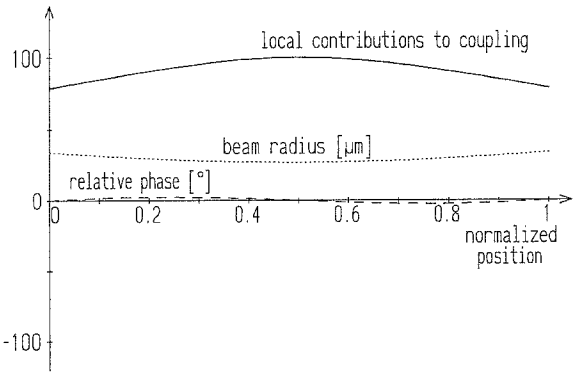

Fig. 1. Local contributions to κ_0 (*solid line*, arbitrary units) in a standing-wave resonator. The horizontal axis gives the normalized position in the resonator. The *dotted line* is the beam radius (in μm). The *dashed line* is the relative phase between fundamental and second-harmonic wave (in degrees), which is optimal at the beam waist and nearly optimal everywhere else

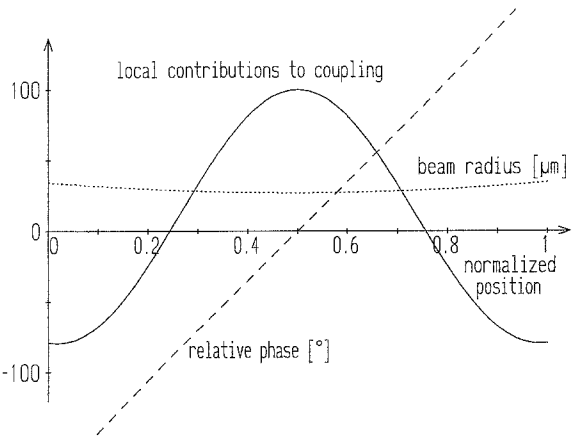

Fig. 2. The same diagram as in Fig. 1, but for κ_2. The relative phase is optimal only near the beam waist. The ends of the resonator give negative contributions, and the resulting nonlinearity is quite small (only 3% compared to κ_0)

The measurement of κ for a monolithic resonator is, in general, not trivial. In our experiments we have developed a method which relies on the back-action of second-harmonic generation on the fundamental wave and also provides information about the losses of the second-harmonic wave. We scanned the resonator through a resonance by the use of an electric field; crystal temperature and laser frequency were adjusted so that resonances of the fundamental and second-harmonic wave coincided. Due to the higher finesse and higher electro-optic coefficient (known from SHG measurements at different temperatures and voltages) of the second-harmonic wave, the peak in the transmitted fundamental intensity had a narrow dip at the centre caused by the losses by SHG (see Fig. 3). The width and height of this dip could be used to determine both the absorption losses of the second-harmonic and the nonlinear coupling. This required the numerical solution of (1) and (2) for arbitrary detunings with the coefficients of absorption and nonlinear coupling as fit parameters.

We have plotted the calculated and the measured pattern of values κ_N as histograms in Figs. 4 and 5 for a monolithic standing-wave resonator made of $MgO:LiNbO_3$, which has

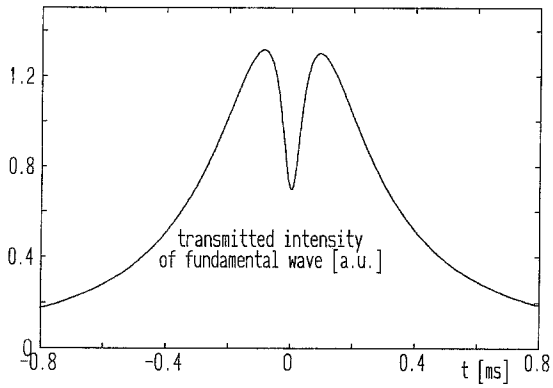

Fig. 3. Intensity of the fundamental wave transmitted by a monolithic standing-wave resonator while the resonator is scanned through a double-resonance with an electric voltage. The dip at the centre is due to losses of the fundamental wave by second-harmonic generation. Curves of this kind have been used for the measurement of the losses of the second-harmonic light and the nonlinear coupling constants

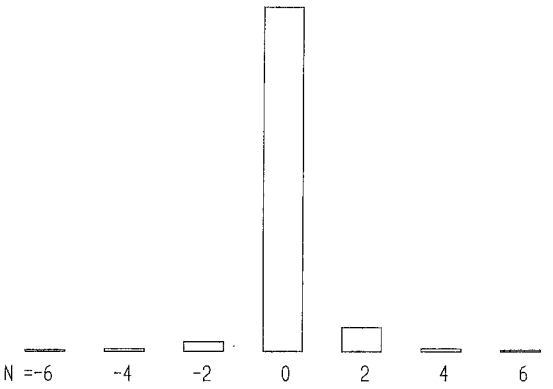

Fig. 4. Calculated nonlinear coupling κ_N as a function of N for our monolithic standing-wave resonator. The phase changes upon reflections are assumed to be zero. The maximum coupling is $\kappa_0 = 24 \times 10^3/\mathrm{s}$. Resonances with odd index have zero coupling

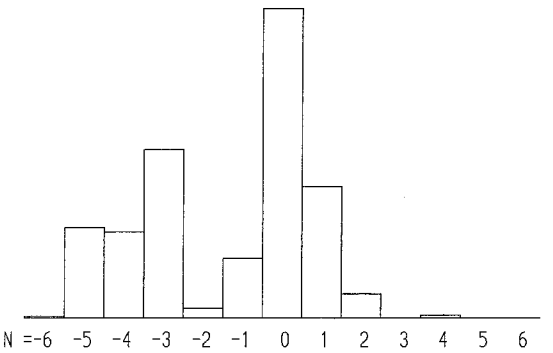

Fig. 5. Measured nonlinear coupling κ_N for our standing-wave resonator (same vertical scale as in Fig. 3). The maximum coupling is $\kappa_0 = 22 \times 10^3/\mathrm{s}$

been used in a squeezing experiment. Zero phase changes at the mirrors are manufacturer specified and are assumed for the theoretical calculation. The focusing was somewhat weaker than required for optimum non-linear coupling in order to keep the beam waist larger; we use $L = 7.5$ mm and $R = 10$ mm, so that $\xi = 0.775$. The figures show that the relative heights of the bars in the patterns are not consistent between theory and experiment, and also the assumption of different phase relations at the mirrors could not explain the experimental result. This shows that there are considerable inhomogeneities in the crystal, though not strong and rapid enough to degrade κ_0 seriously: κ_0 is only by 10% lower than predicted. It might also be that the nonlinearity of the material is slightly higher than given in literature for similar materials (the histogram in Fig. 4 was calculated with $d_{\mathrm{eff}} = 4.7$ pm/V [17]). It is clear that because of the observed phase changes due to inhomogeneities, the optimization of the phase properties of the mirrors is irrelevant.

To our knowledge it was for the first time that the nonlinearity in a doubly resonant frequency doubler has nearly reached the theoretical limit; in our earlier experiments as well as in experiments done by other groups [8] the experimental values were too low by more than a factor 3, sometimes by more than one order of magnitude. Both the use of the best material and special care at the production process of the mirror coatings, done in the Laser Zentrum Hannover, was crucial.

2.2 Monolithic Ring Resonator

The second system which we have investigated is a MOTIRR (MOnolithic Total Internal Reflection Resonator), a monolithic ring resonator, where the modes are confined by total internal reflection and input/output coupling is achieved by frustrated total internal reflection with prisms approached to the crystal to within a few hundred nanometers. This resonator concept has been explained in detail in [5, 19, 20]. Recently, we have demonstrated efficient frequency doubling at power levels of a few milliwatts with such a device [5]. Its high versatility and flexibility results mainly from the fact that one can adjust input and output coupling for the fundamental and second-harmonic wave independently by varying the air gaps between the prisms and the crystal.

The calculation of κ_N for the MOTIRR differs from that for the standing-wave resonator in a few points. We have now four paths instead of two forming one round trip, and there is no significant spatial overlap between those paths. The phase relations between the paths are governed by the boundary conditions at the total internal reflection. It is important to note that fundamental and second-harmonic wave differ in polarization; the polarization vector of the fundamental mode lies in the plane of the ring (p-polarization), whereas for the second-harmonic mode it is perpendicular to the ring (s-polarisation). The phase changes for p-polarized and s-polarized waves are given by [21]

$$\tan \delta_{\mathrm{p}}/2 = -\left(\sin^2\phi - \frac{1}{n^2}\right)^{1/2} \Big/ \left(\frac{1}{n^2}\cos\phi\right) \quad \text{(fundamental wave)}, \tag{14}$$

$$\tan \delta_{\mathrm{s}}/2 = -\left(\sin^2\phi - \frac{1}{n^2}\right)^{1/2} / \cos\phi \quad \text{(second-harmonic wave)}, \tag{15}$$

and thus known in our experiment. The angle of incidence is $\phi = 45°$. We have neglected the small influence of the coupling prisms on the phase changes. Deviations between

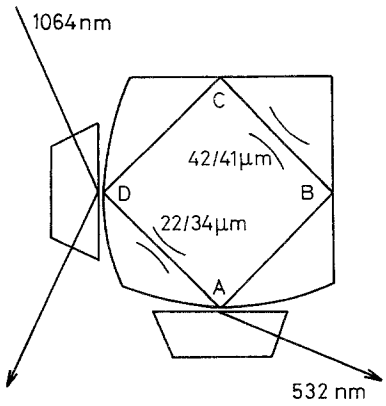

Fig. 6. Beam path in the MOTIRR with two beam waists (beam radii in both directions given for the fundamental wave). Crystal length is 5 mm. The two prisms are approached to the crystal to a distance of a few hundred nanometers

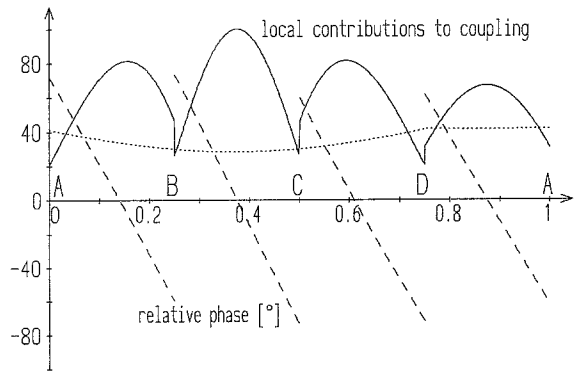

Fig. 7. Local contributions to κ_0 (*solid line*, a.u.) in the MOTIRR. The letters along the x axis denote the positions as defined in Fig. 6. The *dotted line* is the mean beam radius (in μm, averaged over both transverse directions). The *dashed line* is the relative phase between fundamental and second-harmonic wave (in degrees). Note the phase jumps upon reflections which prevent the relative phase from being optimal all over the crystal

the measured and calculated pattern of κ_N can be explained only by inhomogeneities in the crystal since there are no other unknown parameters.

Another difference to the standing-wave resonator is that the modes are astigmatic; this is due to the reflection at the two spherically curved surfaces of the crystal under oblique incidence. It can be shown that the effect of the astigmatism causes the factor $(1+\mathrm{i}\tau)^{-1}$ in (12) to be replaced by $[(1+\mathrm{i}\tau\beta)(1+\mathrm{i}\tau/\beta)]^{-1/2}$, where $\beta = w_{0x}/w_{0y}$ is the ratio of the beam waists in the two perpendicular directions, and we replace w_0 by $(w_{0x}w_{0y})^{1/2}$ everywhere.

Our MOTIRR has two curved sides (neighbouring each other, $R = 19$ mm) and two flat sides, each 5 mm long. The beam has two astigmatic focal points (see Fig. 6); Fig. 7 shows the mean beam radius w_0 along the four paths in the crystal, together with relative phases and the local contributions to κ for $N = 0$. Each path leads to an integral of the form [20]

$$\int \frac{\mathrm{e}^{\mathrm{i}\sigma\tau}}{[(1+\mathrm{i}\tau\beta)(1+\mathrm{i}\tau/\beta)]^{1/2}}\,\mathrm{d}\tau\,, \tag{16}$$

and we have to add phase factors according to the relative phase changes given in (14) and (15).

The experimental determination of κ is somewhat difficult, basically because of the thermal drift of the size of the air gaps between crystal and prisms. We have tried two different methods to solve the problem. First, we determined the conversion efficiency of the device with optimized adjustment of the prisms. The second method was similar to the one applied for the standing-wave resonator which was explained above. Here we used two prisms which couple only the fundamental wave. The first prism was kept at a relatively large distance from the crystal, so that the fundamental losses were dominated by the second prism, used as output coupler to detect the circulating power and the dip occurring at the onset of second-harmonic generation. The width and height of the total peak and of the dip were used to determine the position of the prisms, the second-harmonic absorption losses and finally the nonlinearity κ. Both methods lead to approximately the same results; the accuracy is estimated to be $\pm 20\%$ in both cases.

The theoretical and experimental result we have obtained for our resonator are given as histograms in Figs. 8 and 9. Note that in theory only every forth double-resonance leads to significant nonlinear coupling; this is due to the interference of the contributions of the four paths in the crystal. In the experiment this structure can be recognized, but again we see significant deviations between theory and experiment, which can be explained by inhomogeneities.

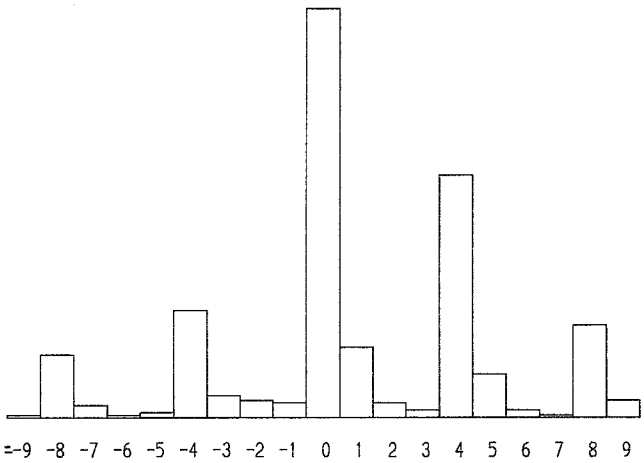

Fig. 8. Calculated nonlinear coupling κ_N for the MOTIRR. The maximum coupling is $\kappa_0 = 17 \times 10^3/\mathrm{s}$. The structure is caused by the interference of the contributions of the four paths in the crystal

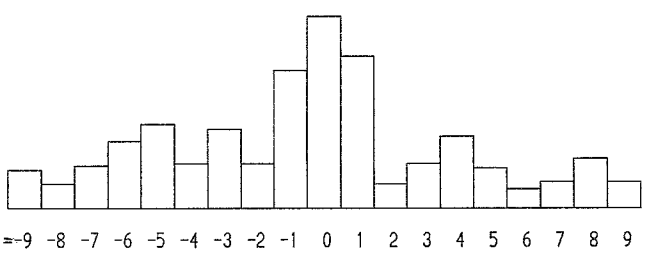

Fig. 9. Measured nonlinear coupling for the MOTIRR (same vertical scale as in Fig. 3). The maximum coupling is $\kappa_0 = 7.9 \times 10^3/\mathrm{s}$. For positive N there is at least some resemblance to Fig. 7. The deviations are due to inhomogeneities in the crystal

Another observation indicating inhomogeneities was that we could excite TEM_{10} transverse modes in the second-harmonic wave, which should normally have zero coupling to all fundamental modes since the integral in (8) vanishes.

In contrast to the case of the standing-wave resonator, the maximum κ is lower than predicted by approximately one half. In addition, the theoretical value is about 30% lower than that for the standing-wave resonator with approximately the same round-trip length, mainly owing to the phase changes at total internal reflection. Although the standing-wave resonator allows for a higher effective nonlinearity, the MOTIRR is still much better than discrete setups (using a crystal and conventional mirrors) with respect to nonlinearity and losses.

3 Conclusion

We have presented the theoretical background for the calculation of the nonlinear coupling constant of doubly resonant frequency doublers in general and discussed in detail two particular cases which have been realized in our experiments. Our theory allows to calculate the strength of the nonlinear coupling for a series of double-resonances; comparison of the pattern of κ_N between theory and experiments provides additional information about the homogeneity of the nonlinear material.

Experimentally we have realized a monolithic frequency doubler in standing-wave geometry which has nearly the full nonlinearity predicted by theory and a very versatile monolithic ring resonator with frustrated total internal reflection which has about 70% of the predicted nonlinearity. Both resonators have considerable inhomogeneities, though not strong and rapid enough to degrade the nonlinear coupling seriously. The optimization of the phase properties of the mirrors is not necessary in this situation, and even in the worst case the wrong phase relations would degrade the nonlinear coupling by about one third only.

Acknowledgements. We greatly acknowledge the support of Stephan Schiller when we constructed our first MOTIRR. R. Henking from the Laser-Zentrum Hannover produced the mirror coatings for our standing-wave resonators. R. P. is supported by the Studienstiftung des Deutschen Volkes. The experiments were funded by the Deutsche Forschungsgemeinschaft and by the European Community under ESPRIT Basic Research Action No. 6934 QUINTEC.

References

1. W.J. Kozlovsky, C.D. Nabors, R.L. Byer: IEEE J. QE-**24**, 913 (1988) and references therein
2. D.H. Jundt, M.M. Feyer, R.L. Byer: Opt. Lett. **16**, 1856 (1991)
3. C. Zimmermann, T.W. Hänsch, R.L. Byer, S. O'Brien, D. Welch: Appl. Phys. Lett. **61**, 2741 (1992)
4. Z.Y. Ou, S.F. Pereira, E.S. Polzik, H.J. Kimble: Opt. Lett. **17**, 640 (1992)
5. K. Fiedler, S. Schiller, R. Paschotta, P. Kürz, J. Mlynek: Opt. Lett. **18**, 1786 (1993)
6. P.D. Drummond, K.J. McNeil, D.F. Walls: Opt. Acta **27**, 321 (1980)
7. P.D. Drummond, K.J. McNeil, D.F Walls: Opt. Acta **28**, 211 (1981)
8. S.F. Pereira, Min Xiao, H.J. Kimble, J.L. Hall: Phys. Rev. A **38**, 4931 (1988)
9. A. Sizmann, R.J. Horowicz, G. Wagner, G. Leuchs: Opt. Commun. **80**, 138 (1990)
10. P. Kürz, R. Paschotta, K. Fiedler, A. Sizmann, G. Leuchs, J. Mlynek: In *Quantum Noise Reduction in Optical Systems*, ed. by E. Giacobino, C. Fabre, Appl. Phys. B **55**, 216 (1992)
11. P. Kürz, R. Paschotta, K. Fiedler, A. Sizmann, J. Mlynek: Europhys. Lett. **24**, 449 (1993)
12. R.J. Horowicz: Europhys. Lett. **10**, 537 (1989)
13. M. Dance, M.J. Collett, D.F. Walls: Phys. Rev. Lett. **66**, 1115 (1991)
14. H.J. Kimble, J.L. Hall: In *Quantum Optics IV*, ed. by J.D. Harvey, D.F. Walls, Springer Proc. Phys., Vol. 12 (Springer, Berlin Heidelberg 1986) pp. 58
15. H. Kogelnik, T. Li: Appl. Opt. **5**, 1550 (1966)
16. G.D. Boyd, D.A. Kleinman: J. Appl. Phys. **39**, 3597 (1968)
17. A. Räuber: In *Current Topics Material Science*, Vol. 1, ed. by E. Kaldis (North-Holland, Amsterdam 1987) pp. 481
18. A. Sizmann, K. Fiedler, P. Kürz, R. Paschotta, J. Mlynek, G. Leuchs: Technical Digest EQEC (1991) p. 145
19. S. Schiller, I.I. Yu, M.M. Feyer, R.L. Byer: Opt. Lett. **17**, 140 (1992)
20. S. Schiller, R.L. Byer: J. Opt. Soc. Am. B **10**, 1696 (1993)
21. M. Born, E. Wolf: *Principles of Optics* (Pergamon, Oxford 1975)